Research Article

Preparation and characterization of a flexible microwave absorber based on MnNiZn ferrite ($Mn_{0.1}Ni_{0.45}Zn_{0.45}Fe_2O_4$) in a thermoset polyurethane matrix

Mais Khadour[1] · **Yomen Atassi**[1] · **Mohammad abdallah**[1]

Received: 5 September 2019 / Accepted: 8 January 2020 / Published online: 19 January 2020

Abstract
In this work, spinel nanoMnNiZn ferrite ($Mn_{0.1}Ni_{0.45}Zn_{0.45}Fe_2O_4$) was hosted by a thermoset polyurethane matrix (PU), to produce flexible thin nanocomposite sheets as efficient microwave absorbers. The microwave absorbers of polyurethane nanocomposites were prepared using different loading ratios of MnNiZn ferrite (70%, 75%, and 80wt%). Microwave absorption properties of the nanocomposites were characterized in the range of S- and C-band (2–8 GHz) frequency. Structural and morphological characterizations were performed using X-ray diffractometry (XRD), Fourier-transform infrared spectrophotometer (FTIR), and scanning electron microscopy (SEM). The tensile test was performed to examine the mechanical properties of the molded nanocomposites. The surface hardness was measured using Shore (A) hardness tool. The nanocomposite with 80 wt% loading percent of ferrite in PU at thickness of 5 mm exhibits the best absorption properties and has effective absorption bandwidth (≥ – 10 dB) of 4.28 GHz, with – 29.7 dB minimum reflection loss (RL) at the matching frequency (5.86 GHz) with density of only 2.403 g/cm^3. The experimental results reveal that the microwave absorption properties of the synthesized nanocomposites were improved and reinforced in the case of polyurethane matrix compared to the paraffin wax matrix, through polar–polar interactions and adhesion between the filler and elastomeric matrix depending on their chemical nature. Also, the effect of thermal aging on the performance of the microwave absorption properties of PU–ferrite nanocomposite has been studied. To the best of our knowledge, the use of this cost-effective thermoset polyurethane matrix prepared from PPG, TDI, and castor oil and loaded with ferrite has not been reported before. The effect of polar–polar interactions between the matrix and the ferrite on the microwave absorption characteristics has also been investigated. The high value of reflection loss makes the obtained lightweight and flexible nanocomposite a promising microwave-absorbing material.

Keywords Spinel ferrite · Thermoset polyurethane · Nanocomposite · Microwave-absorbing material · Reflection loss · Thermal aging

1 Introduction

The increasing number of electromagnetic devices functioning at high frequencies causes harmful electromagnetic waves interference that affects our daily life [1, 2]. Therefore, microwave absorbers have important applications in military and civilian fields [3], such as stealth technology for aircrafts, warships, tanks and anechoic chambers [4], electromagnetic interference shielding (EMI), and protection of the human health from over exposure to electromagnetic emissions in the gigahertz range [5]. Microwave absorbers can be produced in different forms such as paints, sheets, foam, and thin films [5]. Usually, microwave absorbers are obtained by the

✉ Yomen Atassi, yomen.atassi@hiast.edu.sy | [1]Department of Applied Physics, Higher Institute for Applied Sciences and Technology, Damascus, Syria.

SN Applied Sciences (2020) 2:236 | https://doi.org/10.1007/s42452-020-2004-0

dispersion of one or more types of absorbing fillers in a polymeric matrix [5]. Absorbing fillers could have dielectric or magnetic loss that depends on frequency of the electromagnetic radiation [6, 7]. Ferrites are a class of technologically important magnetic materials with interesting magnetic characteristics [8]. NiZn spinel ferrites are the most versatile magnetic materials for general use. They exhibit low magnetic coercivity, high electrical resistivity, high Curie temperature, good mechanical hardness, and high chemical stability [9]. Ferrites can be combined with many conventional polymers to obtain nanocomposites with excellent properties as they impart the desired properties of both components [10]. The high surface area of nanofiller facilitates better interfacial interaction with the matrix and effective load transfer between the polymer and filler [11]. The choice of polyurethane as an elastomeric matrix is due to its favorable properties. PU is a unique material that offers the elasticity of rubber combined with the toughness and durability of metals [12], and excellent adhesion to various substrates [13]. Moreover, PU has better degradation stability than natural rubber and superior mechanical stability than silicone rubber [14]. It can be used for aeronautical and naval applications, because of its excellent resistance to aging, water, and favorable flame-retardant behavior [13]. Thermosetting PU is generally stronger than thermoplastic one due to the three-dimensional network of bonds (cross-linking) and is also better suited to high-temperature applications [15]. The advantages of this composite over their metallic and ceramic counterparts include low weight, resistance to corrosion, ease of machining and forming, and capability for high production rates [16]. Several works have studied polymer-based composites with magnetic filler materials. Gultom et al. studied polyurethane filled with nanozeolite and ferric oxide, loading percent of 20wt%. Binding of zeolite with PU increased the mechanical properties. The nanocomposite absorbs microwave at X-band frequency. The optimized absorber has a thickness of 5 mm, reflection loss of − 13.2 dB at 11.1 GHz [17]. Hsiung Penga et al. prepared $Ni_{0.5x}Zn_{0.5x}CO_{2x}Fe_2O_4$ ($x=0$ or 0.05) ferrite and mixed it with thermoplastic polyurethane (TPU) elastomer. The reflection loss was measured in a frequency range of 2–12 GHz. The best NiZn ferrite–TPU composites absorbed − 20 dB, at thickness of 5 mm, loading percent of 80 wt%, and matching frequency at 5.14 GHz, with effective absorption bandwidth (≥ − 10 dB) equal to 0.57 GHz [18]. Bhattacharyya et al. reported the synthesis of $Mg_{0.5}Zn_{0.5}Fe_2O_4$ (MZF) followed by fabrication of thin layer (~ 100 µm) of ferrite–TPU nanocomposite, which was taken in 1:1 weight ratio. The absorption properties over the microwave frequency range of 4–15 GHz were studied, and the nanocomposite coating showed excellent broadband absorption properties with minimum reflection loss higher than 88% [19]. Tripathi et al. performed a simulation study for metal-backed MWCNT+$Ni_{0.5}Zn_{0.5}Fe_2O_4$/PU nanocomposite single layered as an absorber and examined the electromagnetic absorption properties for different thicknesses (1, 2, 3 mm) of the sample. This nanocomposite was studied at S-, C- and X-band frequencies. For the nanocomposite sample with 35wt% NiZn ferrite, 15 wt% multi-wall carbon nanotubes (MWCNT), and 50wt% TPU, the minimum reflection loss was − 12 dB, at the matching frequency of 7.9 GHz at 2.0 mm thickness, with effective absorption bandwidth (≥ − 10 dB) equal to 1.5 GHz [20]. Abbas et al. have studied microwave absorption properties of ferrite ($BaCo_{0.9}$ $Fe_{0.05}$ $Si_{0.95}$ $Fe_{10.1}$ O_{19})–PU composite at different ferrite ratios of 50%, 60%, 70%, and 80wt% in PU matrix, in the X-band (8.2–12.4 GHz) frequency range. The reflection loss at various sample thicknesses was studied. The composite with 80wt% ferrite content has shown a minimum reflection loss of −24.5 dB at 12 GHz with the effective absorption bandwidth (≥ − 20 dB) of 2 GHz for an absorber thickness of 1.6 mm [21]. Gupta KK et al. have studied microwave properties at 8–18 GHz frequency of the cotton fabric samples coated with 40 wt% ferrite, 3 wt% carbon, and 57 wt% PU at thickness of 1.6–1.8 mm. The samples have shown about 40% absorption, 20% transmission, and 40% reflectance in X and Ku frequency bands. The reflection loss at 13.5 GHz has shown the highest peak value (− 22.5 dB) and more than − 7.5 dB in entire Ku band [22]. Dias JD et al. prepared formulations of PU resin loaded with carbon black and NiZn ferrite. Measurements of different coating formulations applied on aluminum flat plates (l.0 mm thickness) were performed in the X-band frequency range. The attenuation values were − 4 dB for the formulation of polyurethane 49wt%/carbon black 1wt%/ferrite 50wt% [23]. In the current work, a new microwave-absorbent nanocomposite was created with a unique combination and properties suitable for absorption in 2–8 GHz frequency range. The aim of this work is to obtain cost-effective, flexible lightweight microwave-absorbing sheets with good mechanical properties and wide-frequency absorption band. The nanocomposites sheets were prepared by dispersion of $Mn_{0.1}Ni_{0.45}Zn_{0.45}Fe_2O_4$ ferrite nanostructures into the polyurethane matrix. The selected castable cross-linked polyurethane matrix can be either molded, coated on substrate owing to its adhesion ability, or sprayed by mixing it with appropriate solvents, along with the other advantages of usual polyurethane. MnNiZn ferrite was introduced into PU matrix by in situ reaction at different loading ratios 70%, 75%, and 80wt%. First, ferrite was dispersed in a mixture of hydroxyl-terminated polyether (PPG) and triol crosslinker (castor oil). Then, aromatic isocyanate (TDI) was added. After casting the high viscous mixture in molds, thermal curing was done to obtain the nanocomposite.

Mechanical properties were studied. The chemical and physical structure and the morphology of the samples were investigated by FTIR, XRD, and SEM. The microwave absorption properties of ferrite–PU nanocomposite were studied at S- and C-bands. The influence of ferrite content and sheet thickness on the microwave absorption properties of the nanocomposites was investigated. The role of the nature of hosting matrix on the microwave absorption behavior is slightly reported in the literature. In the current study, the role of hosting matrix and its chemical nature in the absorption process are highlighted and compared to the results obtained in paraffin. Polymers are susceptible to chemical degradation under exposure to various conditions which leads to changes in polymer physical and mechanical properties. In this respect, the accelerated thermal aging of the nanocomposite samples has been studied at 75 °C and 125 °C in air atmosphere.

2 Experimental

2.1 Materials

Poly(propylene glycol) (PPG, Mn 2000 g/mol), triphenyl bismuth (TPB), and 2, 4-toluene diisocyanate (TDI) were purchased from Sigma-Aldrich. Castor oil (cross-linking agent) was purchased from Chengdu, China. All these materials have been used as received.

2.2 Synthesis of MnNiZn ferrite powder

The $Mn_{0.1}Ni_{0.45}Zn_{0.45}Fe_2O_4$ spinel ferrite was prepared by conventional method as reported elsewhere. The metal oxides are mixed stoichiometrically using ball mill. Then, a heat treatment is done at the rate of 10°/min until 1100 °C for 3 h. Then, the resulted ferrite is re-milled for 2 h.

2.3 Preparation of PU–ferrite nanocomposite

PU is generally synthesized from an isocyanate reaction with polyol at specific stoichiometric ratio. The PU–ferrite nanocomposites are prepared by mechanical blending method.

The ratio of free isocyanate group to free hydroxyl group should be NCO/OH≥1 to obtain cross-linked polyurethane. Firstly, all polyols were dehydrated at 100 °C under vacuum for 3 h prior to use, and ferrite powder was dried in vacuum oven at 80 °C for 3 h to evict moisture. Then, castor oil was mixed with PPG in the presence of a catalyst triphenyl bismuth (TPB). Secondly, ferrite powder was added (at the concerned loading percent) gradually into polyol mixture with high-speed mechanical stirring at 75 °C until forming homogenous mixture. After that, diisocyanate was added to the polyol mixture under vacuum degassed to avoid water vapor since the reaction, which is sensitive to moisture, and at high-speed stirring for 20 min at 75 °C. Finally, the mixture was casted and then cured at 85 °C for 24 h.

2.4 Preparation of wax–ferrite nanocomposite

Ferrite was mixed in paraffin matrix at a weight ratio of 70wt%. Ferrite powder was added into the molten paraffin and homogenized well using ultrasonic vibration for 10 min and then molded using a hydraulic press. Table 1 presents the prepared samples with its precise composition.

3 Characterization techniques

The microstructure and the morphology of the samples were characterized by X-ray diffraction (Philips, X'pert using a Cu Kα source, λ=0.1542 nm over a scan range of 10°–70° in steps of 0.02°/s) and scanning electron microscopy (VEGA II TESCAN), respectively. The bonding interactions were studied using Fourier-transform infrared spectrometer (FTIR) (Bruker, Vector 22 spectrophotometer, using KBr pellets (400–4000 cm^{-1})). Mechanical properties were studied using the universal testing machine (DY-34 Adamel Lhomargy, France) of 1 kN load capacity at 25 °C. Hardness was measured using Shore A durometer (hardness testing apparatus following ASTM D-882). The reflection loss (RL) of

Table 1 Prepared compositions of PU–ferrite and pure PU samples

Material	Pure PU (wt%)	PU–70 wt% ferrite	PU–75 wt% ferrite	PU–80 wt% ferrite
PPG	77.75	23.325	19.437	15. 55
Castor oil	11	3.3	2.75	2.2
TDI	11	3.3	2.75	2.2
TPB	0.25	0.075	0.063	0.05
Ferrite	–	70	75	80

nanocomposite materials was obtained by a vector network analyzer (VNA, R&S, FSH4/FSH8), in the frequency range of S–C bands (2–8 GHz). For thermal aging studies, PU–ferrite samples have been placed in an oven at 75 °C and 125 °C in air atmosphere for 2000 min. RL tests were realized on these samples during the time of aging.

4 Results and discussion

4.1 Structural characterization

XRD Fig. 1 depicts the XRD patterns of the PU, magnetic ferrite powder, and PU–ferrite nanocomposite. For pure PU in Fig. 1a, there is only one broad diffraction peak at 2θ = 21.5°, caused by the crystallization of chain segments (soft segments).

XRD diffraction peaks of $Mn_{0.1}Ni_{0.45}Zn_{0.45}Fe_2O_4$ spinel ferrite in Fig. 1b are obtained at 30.8°, 35.6°, 43°, 53.2°, 57°, and 62.3°, which are related to the single cubic spinel phase [24]. The particle size was measured by Scherer's formula [25], using half width of the (311) peak. The calculated particle size is about 157 nm.

$$D = \frac{0.9\lambda}{\beta\cos(\theta)}$$

where D is the mean crystallite size, β is the half width of the relevant diffraction peak, λ is the X-ray wavelength, and θ is the angle of peak.

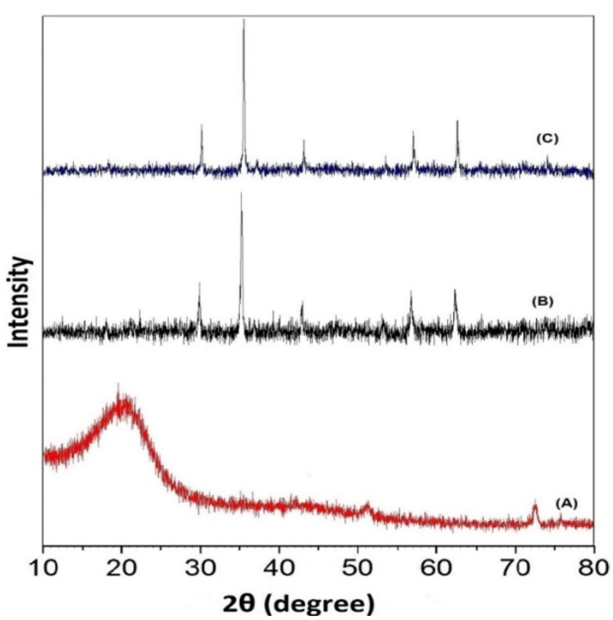

Fig. 1 (a) XRD pattern of pure PU, (b) XRD pattern of $Mn_{0.1}Ni_{0.45}Zn_{0.45}Fe_2O_4$ spinel ferrite, (c) XRD pattern of PU–ferrite nanocomposite

XRD pattern of the nanocomposite in Fig. 1c shows all ferrite diffraction peaks, with the absence of PU crystallization peak. The absence of PU peak can be attributed to high amount of ferrite filler that extends the polymer chain network, decreases the interactions among urethane groups, and eventually reduces the crystalline regions.

FTIR Fig. 2 presents the FTIR spectrum of the spinel ferrite sample. In this spectrum, there are two absorption bands around 582 cm^{-1} and 415 cm^{-1} which are attributed to Fe–O stretching vibration in tetrahedral and octahedral sites of the spinal structure, respectively [24].

The FTIR spectrum of PU after one day of thermal curing is presented in Fig. 3a. The band around 3320 cm^{-1} corresponds to the free and bonded N–H stretching vibrations of urethane. The absorption peak of C–N–H bending locates at 1528 cm^{-1}. The band at 2900 cm^{-1} is due to C–H stretching. The non-bonded urethane carbonyl (C=O) stretching is seen at 1733 cm^{-1}. The peak at 1598 cm^{-1} is assigned to the aromatic ring in polyurethane structure. The absorption peak at 2350 cm^{-1} is assigned

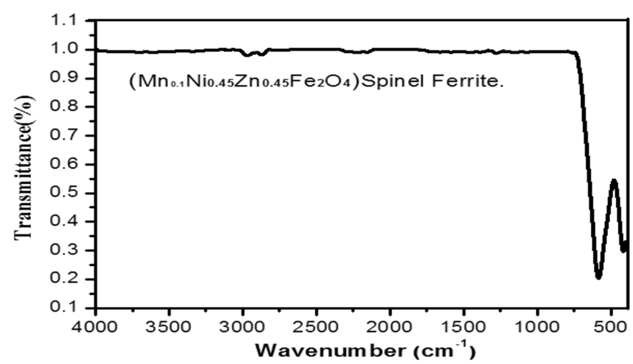

Fig. 2 FTIR spectrum of $Mn_{0.1}Ni_{0.45}Zn_{0.45}Fe_2O_4$ spinel ferrite

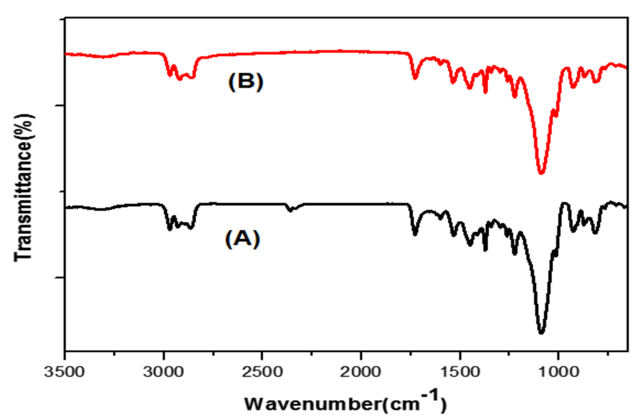

Fig. 3 FTIR spectra of (a) pure PU after one day of thermal curing and (b) pure PU after 6 months of thermal curing

to the N=C=O group. Finally, the peak of C–O–C bending is located at 1090 cm^{-1} [26].

FTIR spectrum of PU after 6 months of thermal curing is presented in Fig. 3b. From comparison with Fig. 3a, it can be observed the disappearance of the absorption peak at 2350 cm^{-1} which is assigned to the N=C=O group of PU, and it confirms the fully cured PU after 6 months, which means that all diisocyanate groups were consumed in the reaction.

FTIR spectra of the nanocomposites in Fig. 4 exhibit the same peaks of PU along with those of ferrite without showing any reaction between the filler (ferrite) and the matrix (PU). In fact, there are no chemical groups in ferrite which can react with PU organic groups. By comparing FTIR spectrum of PU–70% ferrite with PU–75% ferrite, and PU–80% ferrite spectra, one can observe that they are similar and the main characteristic peaks of PU and ferrites are present. It is difficult to conclude that there is an increase in the relative intensity of ferrite's peaks compared to peaks of PU with the increase in ferrite's loading percentage.

4.2 Morphological properties

SEM micrographs of spinal ferrite are shown in Fig. 5a and b. One can easily observe the grains with lamellar structure of average diameter of 500 nm. SEM micrograph of PU–ferrite is shown in Fig. 5c and d. These figures show the regular dispersion of ferrite particles in the polyurethane matrix.

4.3 Mechanical properties

4.3.1 Tensile strength test

The tensile tests were performed for the pure PU, PU–70% ferrite, PU–75% ferrite, and PU–80% ferrite nanocomposites. The results are shown in Fig. 6. Pure PU has rubbery behavior. One can observe that the PU matrix exhibits good elasticity as shown in Fig. 6a.

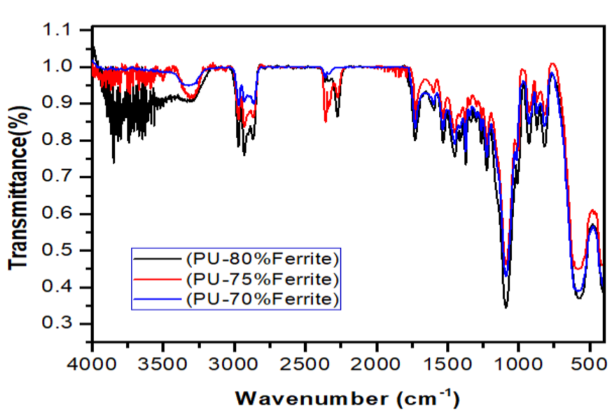

Fig. 4 FTIR spectra of PU– 80,75,70% ferrite nanocomposites

The PU–ferrite nanocomposites showed viscoelasticity behavior. Mechanical properties were enhanced by incorporation of ferrite into an elastomeric matrix. Compared with pure PU, the maximum tensile stress and Young's modulus of nanocomposites have increased, whereas the elongation at break (%) has decreased, as shown in Fig. 6. On the other hand, with increasing ferrite weight percentage in the PU–ferrite nanocomposites, the maximum tensile stress and Young's modulus have increased, whereas the strain tensile has reduced. The PU–80% ferrite nanocomposite showed the highest tensile stress and Young's modulus and the lowest elongation at break (%) compared with PU–70% ferrite and PU–75% ferrite as shown in Fig. 7. The elasticity nature of the fabricated samples are shown in Fig. 8.

4.3.2 Hardness test

The Shore A hardness of PU–ferrite nanocomposites and pure PU was measured. The results are listed in Table 2. These results indicate that the hardness of the rubbery polyurethane has increased significantly when it is loaded with ferrite, and the hardness has increased with increasing loading percentage, as shown in Fig. 7d, making the nanocomposite an engineering material suitable for many applications.

4.4 Microwave measurement

The reflection loss of an electromagnetic radiation from a surface of a monolayer microwave absorber is given in Equation [5]:

$$R(\mathrm{dB}) = 20\log\left|\frac{Z_{in} - Z_0}{Z_{in} + Z_0}\right|$$

where Z_0 represents the free-space intrinsic impedance and Z_{in} is the input impedance of the layer.

The reflection loss of the pure polyurethane at different thicknesses (4, 6 mm) is shown in Fig. 10. It is clear that polyurethane is an insulating material, which does not absorb electromagnetic radiation. This can be explained by the absence of both electrical and magnetic dipoles in the polyurethane structure and its low polarity. The reflection loss plot of the nanocomposites (PU–ferrite) with different loading percent (70%, 75%, and 80wt%) and different thicknesses in the S- and C-band region is shown in Fig. 9b, c, and d. It can be seen from Fig. 10c that the matching frequency of the nanocomposite materials shifts to the higher frequencies when the materials thickness decreases. And that corresponds to the following

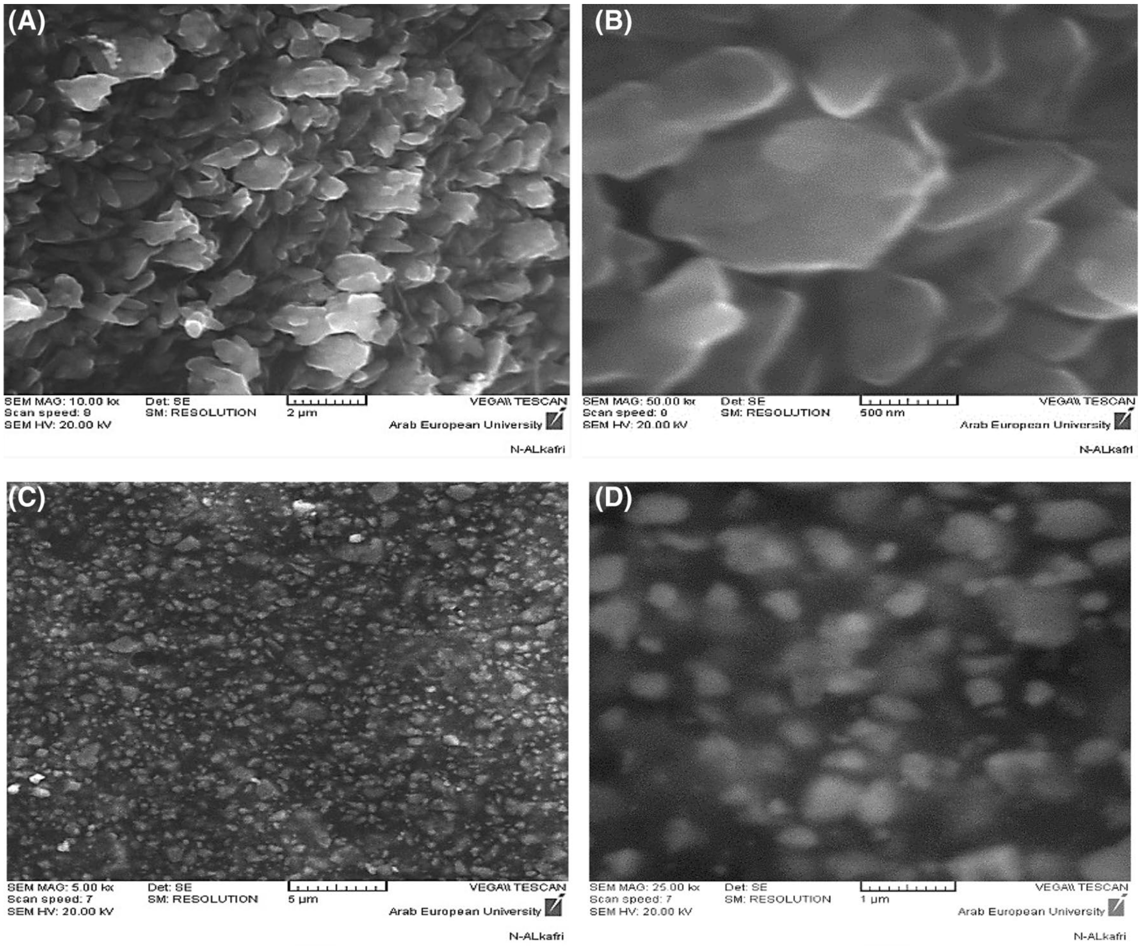

Fig. 5 Scanning electron micrographs of (**a** and **b**) $Mn_{0.1}Ni_{0\cdot45}Zn_{0\cdot45}Fe_2O_4$ spinel ferrite, (**c** and **d**) PU–ferrite nanocomposite

equation, which relates between matching frequency and absorber thickness:

$$t_m = \frac{c}{4f\sqrt{|\varepsilon_r||\mu_r|}}$$

where f represents the matching frequency, t_m is the absorber thickness, ε_r is the relative complex permittivity, and μ_r is the relative complex permeability.

From Fig. 9b, it can be observed that the nanocomposite with 70wt% of loading percentage and density 2.038 g/cm^3 and 6 mm thickness exhibits the best microwave absorption performance with 4 GHz effective absorption bandwidth (≥− 10 dB), and minimum reflection loss of − 19.9 dB at 5.6 GHz. From Fig. 9c, it can be easily seen that the nanocomposite with 75wt% of loading percentage and density of 2.226 g/cm^3 and 5.5 mm thickness exhibits the best absorption performance with more than 4 GHz effective absorption bandwidth (≥− 10 dB), and minimum reflection loss of − 23.15 dB at 5.71 GHz. For the nanocomposite with 80 wt% of loading percentage and density of 2.403 g/cm^3 and the thickness of 5 mm exhibits the best absorption performance with more than 4.17 GHz effective absorption bandwidth (≥ − 10 dB), and minimum reflection loss of − 29.7 dB at 5.86 GHz; also, the PU–80% ferrite nanocomposite exhibits microwave absorption peak at low thicknesses, 6.5 GHz with 2.94 GHz effective absorption bandwidth (≥ −10 dB) and minimum reflection loss of − 14 dB of 4 mm, and 6.6 GHz with 2.55 GHz effective absorption bandwidth (≥ − 10 dB) and minimum reflection loss of − 13.8 dB for thickness of 3.75 mm, as shown in Fig. 9d. This is due to the magnetic loss properties of the MnNiZn ferrite and the role of the polymeric matrix in enhancing the microwave absorption. So, the effective absorption bandwidth (≥− 10 dB) and minimum reflection loss increase with the increasing loading percentage of ferrite, whereas the matching frequency shifts toward low frequencies for the same thickness of the prepared nanocomposites, as shown in Fig. 10.

For studying the effect of the polymeric matrix on the microwave absorption properties of the ferrite, samples of wax–70% ferrite nanocomposite were prepared. The

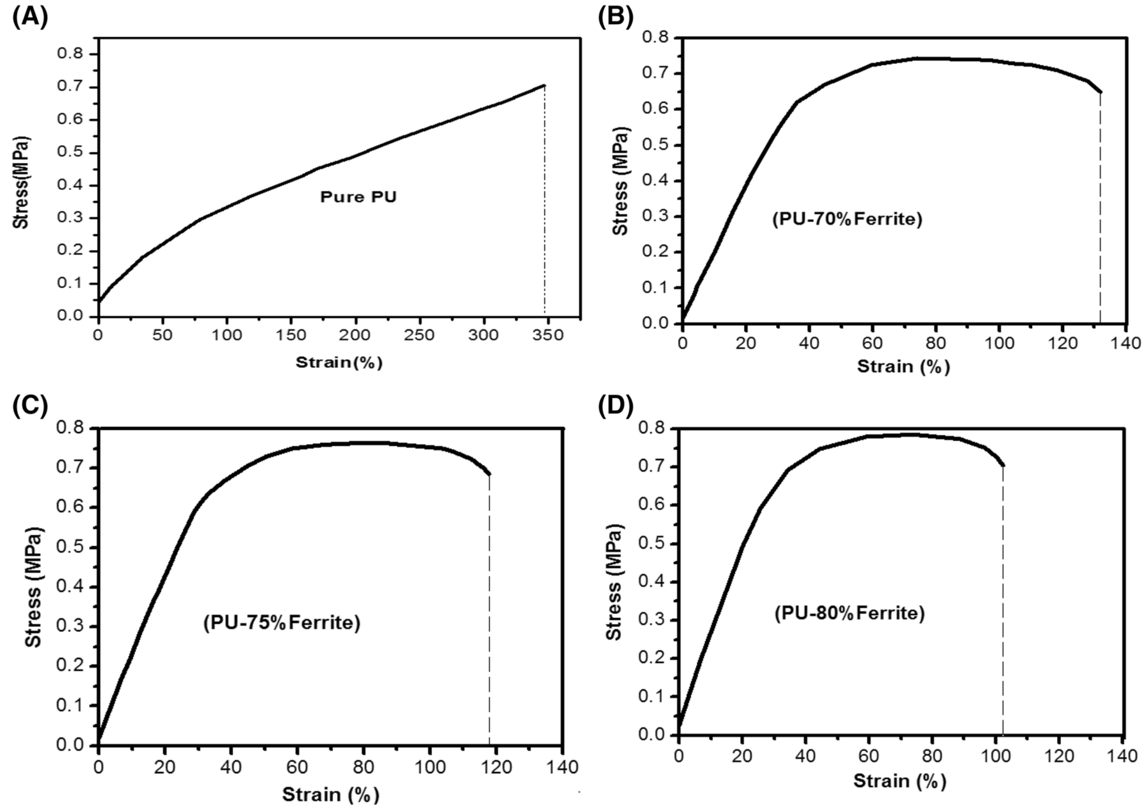

Fig. 6 Tensile test (stress–strain) curves of **a** pure PU, **b** PU–70% ferrite, **c** PU–75% ferrite, and **d** PU–80% ferrite nanocomposites

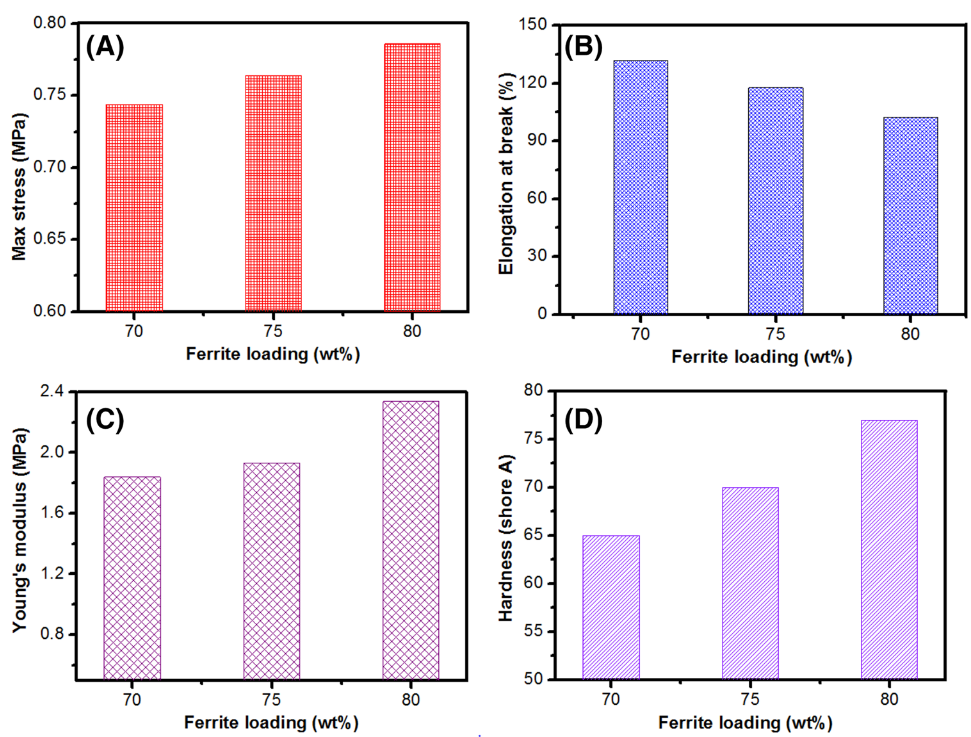

Fig. 7 **a** Max stress values, **b** elongation at break (%) values, **c** Young's modulus values, **d** hardness (Shore A) values of PU–ferrite nanocomposites

microwave absorption characteristics of wax-70% ferrite and PU-70% ferrite nanocmposites are summarized in Table 3.

The comparison between the reflection loss results of PU–70% ferrite nanocomposite with wax–70 wt% ferrite is depicted in Fig. 11a and b. The results show that the effective absorption bandwidth (≥ – 10 dB) for the samples based on polyurethane matrix is wider than the samples based on wax matrix for the same thickness. One can also observe a slight shift toward lower frequencies in the case of polyurethane matrix. The increase in the bandwidth suggests that the polyurethane matrix reinforces the performance of the absorbing material owing to the polar–polar interfacial interactions between the polymeric matrix and the absorbent material [8]. This novel type of dielectric polarization may contribute in increasing the values of double-prime epsilon ε″ responsible for dielectric loss in the material.

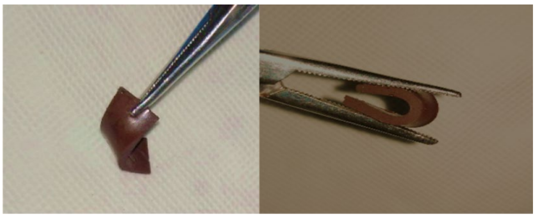

Fig. 8 Images of fabricated PU–ferrite nanocomposite showing its elasticity nature

Table 2 Tensile and hardness test results of PU–ferrite nanocomposite and pure PU

	Pure PU	PU–70% ferrite	PU–75% ferrite	PU–80% ferrite
Ultimate tensile stress (MPa)	0.705	0.743	0.764	0.787
Elongation at break (%)	346.5	131.9	117.8	102.2
Young's modulus (MPa)	0.316	1.84	1.93	2.337
Hardness (Shore A)	28	65	70	77

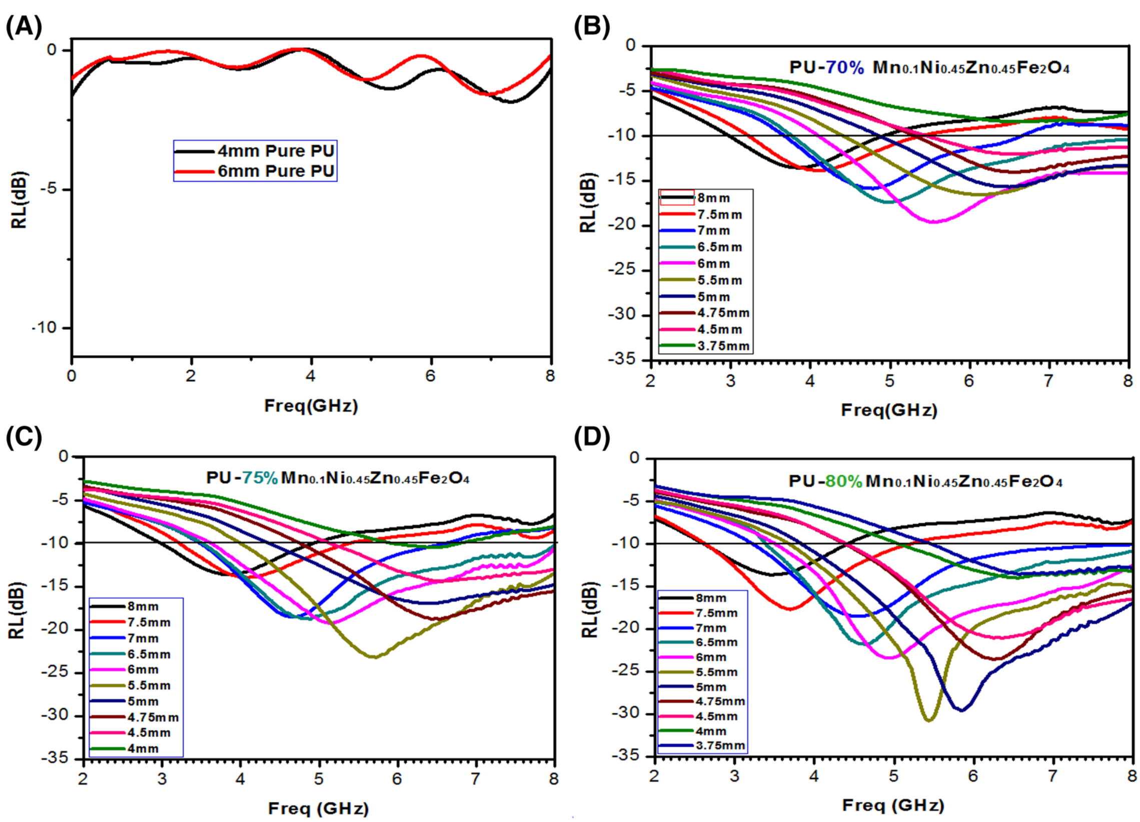

Fig. 9 RL curves of **a** pure polyurethane, **b** PU–70% ferrite, **c** PU–75% ferrite, and **d** PU–80% ferrite nanocomposites

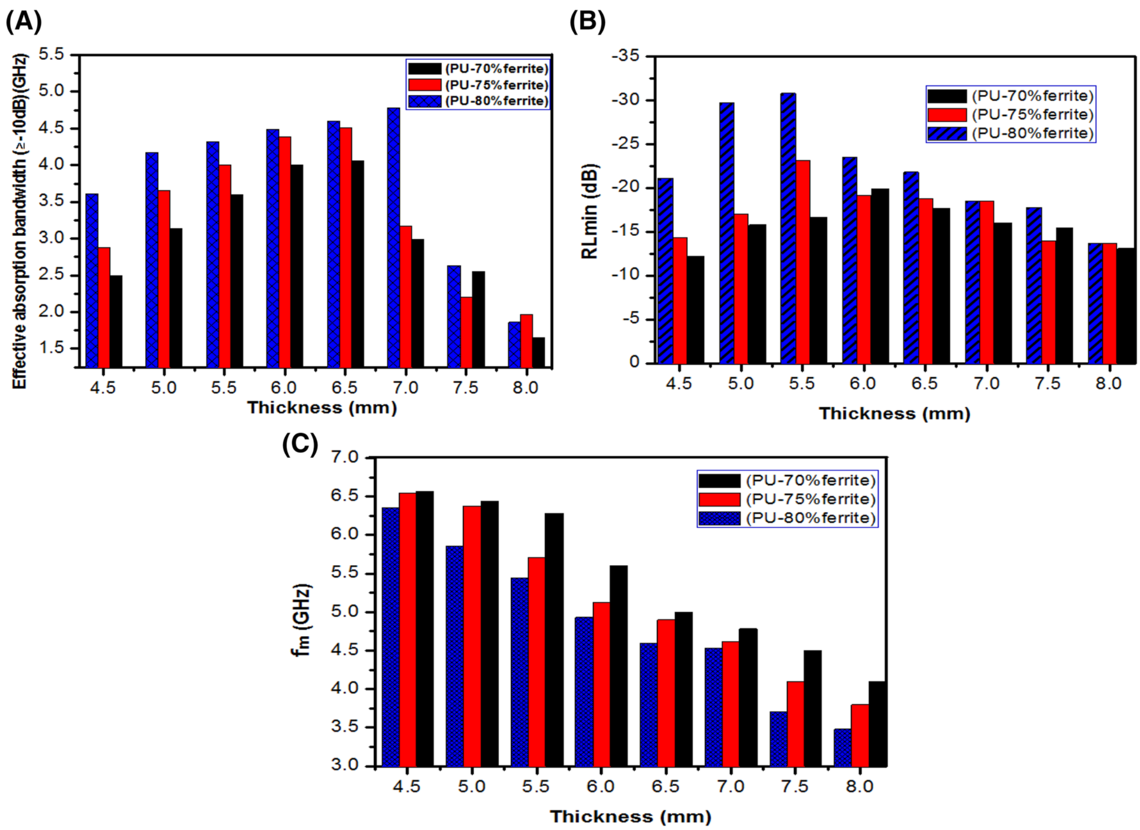

Fig. 10 **a** Effective frequency bandwidth (≥ − 10 dB) values, **b** RL_{min} peak values, and **c** matching frequency values of PU–ferrite nanocomposites

Table 3 The reflection loss results of wax–70 wt% ferrite and PU–70% ferrite nanocomposites

Absorber thickness	Minimum reflection loss (dB)		Effective absorption bandwidth (≥ − 10 dB)(GHz)		Matching frequency (GHz)	
	Wax–70% ferrite	PU–70% ferrite	Wax–70% ferrite	PU–70% ferrite	Wax–70% ferrite	PU–70% ferrite
6.5 mm	− 17.57	− 17.7	2.75	4.06	5	5
6 mm	− 18.36	− 19.9	3	4	5.6	5.6
5.5 mm	− 17.9	− 16.6	3.3	3.6	6.23	6.28

4.5 Effect of thermal aging on microwave absorption performance

Figure 12a and b depicts the variation of RL during accelerated thermal aging, (A) at 75 °C and (B) at 125 °C of PU–ferrite nanocomposite. One can see the high stability of the microwave absorption property of PU–ferrite nanocomposite during the aging at the two temperatures. The PU–ferrite samples had the same matching frequency and the same intensity and bandwidth for all measurement during the aging time. This high stability is due to the great thermal stability of the ferrite. The decrease in elasticity of the samples was observed during accelerated thermal aging, especially samples aging at 125 °C due to increased urethane groups because of the reaction of isocyanate and hydroxyl-free groups causing increased crosslinking, molecular weight, rigidity, and also the breakage of chains due to oxidation reactions which is generally one of the most common problems encountered during the use of polymers, especially at high temperatures. One can conclude that the aging of the matrix does not affect the performance of the ferrite as a microwave absorber.

In order to assess the performance of the current microwave absorber, a comparison with similar absorbers is shown in Table 4. From comparison with the other results, one can readily deduce that the current microwave absorber

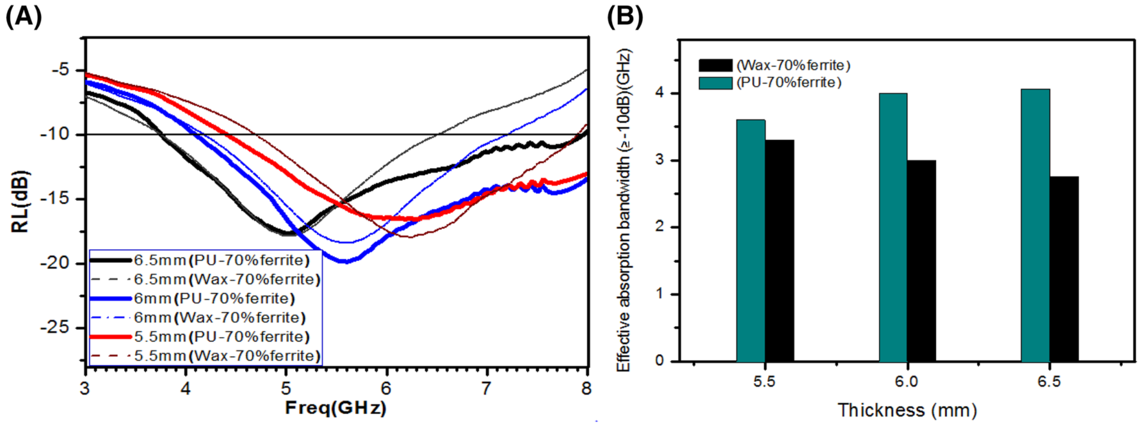

Fig. 11 **a** The reflection loss of wax–70% ferrite and PU–70% ferrite nanocomposites, **b** effective absorption bandwidth (≥ – 10 dB) values of wax–70% ferrite and PU–70% ferrite nanocomposites

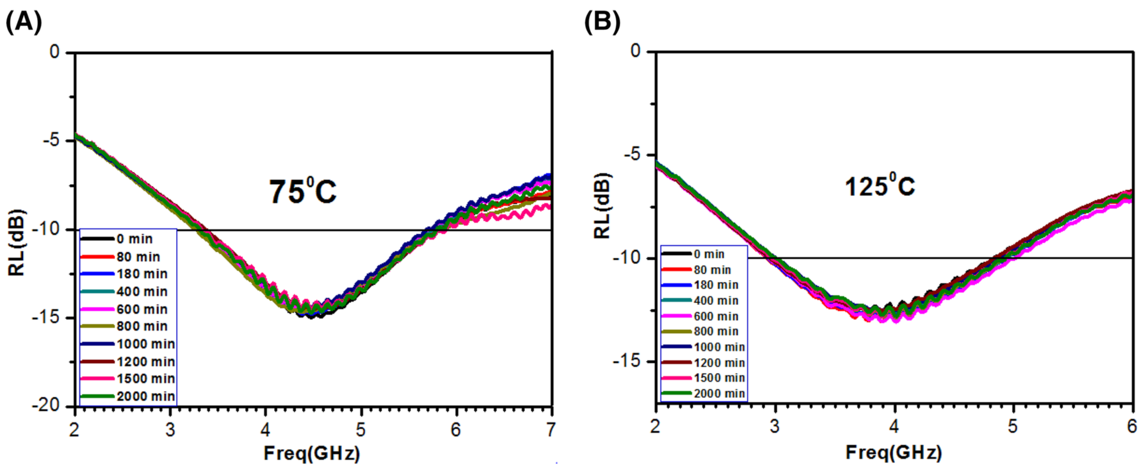

Fig. 12 Reflection loss at accelerated thermal aging during 2000 min at **a** 75°C and **b** 125°C of PU–ferrite nanocomposite

is promising in terms of its broad bandwidth and minimum RL along with its thermosetting nature that confers better suitability to high-temperature applications.

5 Conclusion

In summary, lightweight, flexible nanocomposites with high-absorption characteristics, wide-frequency band, and small specific gravity were developed by incorporation of spinel ferrite into the thermoset polyurethane matrix. Their structural, morphological, mechanical, and microwave properties were investigated. Structural and morphological studies confirmed the presence of ferrite particles in the PU matrix. From mechanical studies, it is suggested that maximum stress, modulus, and hardness enhanced with filler loading onto the host matrix. Microwave absorption properties were analyzed using the vector network analyzer for PU nanocomposites with 70, 75, and 80% filler loading. Due to the magnetic loss properties of the MnNiZn ferrite which were enhanced by the polar–polar interfacial interaction with the thermoset PU matrix, the PU–70% ferrite nanocomposite of only 2.038 g/cm^3 exhibited a good absorption peak at – 19.9 dB (5.6 GHz) with 4 GHz effective absorption bandwidth (≥ – 10 dB) for 6 mm sample thickness. For the case of PU–75% ferrite nanocomposite of 2.226 g/cm^3, the best peak was noted to be – 23.15 dB (5.71 GHz) with 4 GHz for 5.5 mm material thickness. Similarly, for PU with 80% ferrite loading with 2.403 g/cm^3, the peak was obtained at – 29.7 dB (5.86 GHz) with 4.17 GHz for a 5 mm sample thickness. In conclusion, PU with 80% ferrite loading showed the best microwave absorption at – 29.7 dB. The high stability in the microwave absorption property of PU–ferrite samples has been established by studying the accelerated thermal aging. Due to its

Table 4 Comparative study between the results of the current work and similar microwave absorbers in the frequency range of 2–8 GHz

Article	Year	Composition	Fm(GHz)	Thickness dm(mm)	RLmin dB))	Effective absorption bandwidth (≥ − 10 dB) (GHz)
Microwave-absorbing characteristics for the composites of thermal-plastic polyurethane (TPU)-bonded NiZn-ferrites prepared by combustion synthesis method [18].	2005	80%(NiZn) ferrite/thermoplastic PU	2.27	5.65	− 31.03	0.73
Mg0.5Zn0.5Fe2O4–polyurethane thin nanocomposites coating as broadband microwave Absorber [19].	2018	50%(MZF) ferrite/TPU		0.100	88%	–
Tunable Twin Matching Frequency (fm1/fm2) Behavior of Ni1−xZnxFe2O4/NBR Composites over 2–12.4 GHz: A Strategic Material System for Stealth Applications [27].	2017	80%(NiZn) ferrite/NBR	4.6	5	− 28	4
Microwave Absorption Properties of MWCNT and NiZn Ferrite Nano-fillers/TPU based Nano-Composites [20].	2015	35% NiZn ferrite, 15% (MWCNT), and 50% (TPU)	7.9	2	− 12	1.5
Effects of Sheet Thickness on the Electromagnetic Wave Absorbing Characterization of Li0.375Ni0.375Zn0.25-Ferrite Composite as a Radiation Absorbent Material [28].	2016	75%LiNiZn–ferrite/chlorinated polyethylene (CPE)	3.55 5.17	8 6	− 17.5 − 28	1.89 3.95
Current work	2019	80%(MZF)ferrite/thermoset PU	5.86	5	− 29.7	4.17

significant and attractive features, the current nanocomposite holds promise for microwave absorption applications.

Compliance with ethical standards

Conflict of interest On behalf of all authors, the corresponding author states that there is no conflict of interest.

Informed consent The authors certify that they have/grant an informed consent.

Research involving human participants and/or animals The authors certify that the current research does not involve human participants and/or animals.

References

1. Lv H, Yang Z, Wang PL, Ji G, Song J, Zheng L, Zeng H, Xu ZJ (2018) A voltage-boosting strategy enabling a low-frequency, flexible electromagnetic wave absorption device. Adv Mater 15:1706343
2. Quan B, Shi W, Ong SJ, Lu X, Wang PL, Ji G, Guo Y, Zheng L, Xu ZJ (2019) Defect engineering in two common types of dielectric materials for electromagnetic absorption applications. Adv Func Mater. https://doi.org/10.1002/adfm.201901236
3. Folgueras LD, Alves MA, Rezende MC (2010) Microwave absorbing paints and sheets based on carbonyl iron and polyaniline: measurement and simulation of their properties. J Aerosp Technol Manag 1:63–70
4. Zeghina S, Wojkiewicz JL, Lamouri S, Belaabed B, Redon N (2014) Enhanced microwave absorbing properties of lightweight films based on polyaniline/aliphatic polyurethane composites in X band. J Appl Polym Sci 131(21):40961
5. Yang RB, Liang WF, Wu CH, Chen CC (2016) Synthesis and microwave absorbing characteristics of functionally graded carbonyl iron/polyurethane composites. AIP Adv 6(5):055910
6. Singh AP, Mishra M, Dhawan SK (2015) Conducting multiphase magnetic nanocomposites for microwave shielding application. In: Gonzalez Estevez JM (ed) Nanomagnetism. One Central Press, Manchester, pp 246–277
7. Lv H, Yang Z, Ong SJ, Wei C, Liao H, Xi S, Du Y, Ji G, Xu ZJ (2019) A flexible microwave shield with tunable frequency-transmission and electromagnetic compatibility. Adv Func Mater 14:1900163
8. Kruželák J, Sýkora R, Dosoudil R, Hudec I (2016) Rubber composites based on polar elastomers with incorporated modified and unmodified magnetic filler. Adv Mater Sci Eng. https://doi.org/10.1155/2016/7242891
9. Raju P, Murthy SR (2013) Preparation and characterization of Ni–Zn ferrite+ polymer nanocomposites using mechanical milling method. Applied Nanoscience 6:469–475

10. Fu S, Sun Z, Huang P, Li Y, Hu N (2019) Some basic aspects of polymer nanocomposites: a critical review. Nano Mater Sci 1(1):2–30
11. Abraham J, Sharika T, George SC, Thomas S (2017) Rheological percolation in thermoplastic polymer nanocomposites. Rheol Open Access 1:1–5
12. Njuguna J, Pielichowski K (2004) Recent developments in polyurethane-based conducting composites. J Mater Sci 39:4081–4094
13. Ghazali S, Islam MR, Akindoyo JO, Beg MD, Jeyaratnam N, Yuvaraj AR (2017) Polyurethane types, synthesis and applications–a review. RSC Adv 6(115):14453–114482
14. Wei B, Gong X, Jiang W (2010) Influence of polyurethane properties on mechanical performances of magnetorheological elastomers. J Appl Polym Sci 116(2):771–778
15. Dodiuk H, Goodman SH (eds) (2013) Handbook of thermoset plastics. William Andrew, Norwich
16. Camargo PH, Satyanarayana KG, Wypych F (2009) Nanocomposites: synthesis, structure, properties and new application opportunities. Mater Res 12(1):1–39
17. Gultom G, Wirjosentono B, Sebayang K, Ginting M (2016) Preparation and characterization of microwave-absorption of sarulla north sumatra zeolite and ferric oxide-filled polyurethane nanocomposites. Proced Chem 19:441–446
18. Peng CH, Hwang CC, Wan J, Tsai JS, Chen SY (2005) Microwave-absorbing characteristics for the composites of thermal-plastic polyurethane (TPU)-bonded NiZn-ferrites prepared by combustion synthesis method. Mater Sci Eng, B 117(1):27–36
19. Bhattacharyya R, Roy S, Prakash O, Singh AP, Bhattacharya TK, Maiti P, Bhattacharyya S, Das S (2019) Mg 0.5 Zn 0.5 Fe 2 O 4-polyurethane thin nanocomposite coating as broadband microwave absorber. SN Appl Sci 1(1):38
20. Tripathi KC, Abbas SM, Sharma RB, Alegaonkar PS, Verma M (2015) Microwave absorption properties of MWCNT and NiZn ferrite nano-fillers/TPU based nano-composites. Int J Adv Res Sci, Eng Technol 2(2):463–468
21. Abbas SM, Dixit AK, Chatterjee R, Goel TC (2007) Complex permittivity, complex permeability and microwave absorption properties of ferrite–polymer composites. J Magn Magn Mater 309(1):20–24
22. Gupta KK, Abbas SM, Goswami TH, Abhyankar AC (2014) Microwave absorption in X and Ku band frequency of cotton fabric coated with Ni–Zn ferrite and carbon formulation in polyurethane matrix. J Magn Magn Mater 362:216–225
23. Dias JD, Martin IM, Rezende MC (2012) Reflectivity of hybrid microwave absorbers based on NiZn ferrite and carbon black. J Aerosp Technol Manag 3:267–274
24. Ali NN, Al-Marjeh RA, Atassi Y, Salloum A, Malki A, Jafarian M (2018) Design of lightweight broadband microwave absorbers in the X-band based on (polyaniline/MnNiZn ferrite) nanocomposites. J Magn Magn Mater 453:53–61
25. Singh AK, Nakate UT (2013) Microwave synthesis, characterization and photocatalytic properties of SnO2 nanoparticles. Adv. Nanopart 2(66):10–4236
26. Alaa MA, Yusoh K, Hasany SF (2015) Synthesis and characterization of polyurethane–organoclay nanocomposites based on renewable castor oil polyols. Polym Bull 72(1):1–7
27. Saini L, Patra MK, Jani RK, Gupta GK, Dixit A, Vadera SR (2017) Tunable twin matching frequency (f m1/f m2) behavior of Ni 1− x Zn x Fe 2 O 4/NBR composites over 2–12.4 GHz: a strategic material system for stealth applications. Sci rep 7:44457
28. Kim DY, Yoon YH, Jo KJ, Jung GB, An CC (2016) Effects of sheet thickness on the electromagnetic wave absorbing characterization of Li 0.375 Ni 0.375 Zn 0.25-ferrite composite as a radiation absorbent material. J Electromagn Eng Sci 16(3):150–158